Measurement of the branching fractions of $\psi(2S) \to 3(\pi^+\pi^-)$ and $J/\psi \to 2(\pi^+\pi^-)$

M. Ablikim,[1] J. Z. Bai,[1] Y. Ban,[11] J. G. Bian,[1] X. Cai,[1] J. F. Chang,[1] H. F. Chen,[17] H. S. Chen,[1] H. X. Chen,[1] J. C. Chen,[1] Jin Chen,[1] Jun Chen,[7] M. L. Chen,[1] Y. B. Chen,[1] S. P. Chi,[2] Y. P. Chu,[1] X. Z. Cui,[1] H. L. Dai,[1] Y. S. Dai,[19] Z. Y. Deng,[1] L. Y. Dong,[1,*] Q. F. Dong,[15] S. X. Du,[1] Z. Z. Du,[1] J. Fang,[1] S. S. Fang,[2] C. D. Fu,[1] H. Y. Fu,[1] C. S. Gao,[1] Y. N. Gao,[15] M. Y. Gong,[1] W. X. Gong,[1] S. D. Gu,[1] Y. N. Guo,[1] Y. Q. Guo,[1] Z. J. Guo,[16] F. A. Harris,[16] K. L. He,[1] M. He,[12] X. He,[1] Y. K. Heng,[1] H. M. Hu,[1] T. Hu,[1] G. S. Huang,[1,†] X. P. Huang,[1] X. T. Huang,[12] X. B. Ji,[1] C. H. Jiang,[1] X. S. Jiang,[1] D. P. Jin,[1] S. Jin,[1] Y. Jin,[1] Yi Jin,[1] Y. F. Lai,[1] F. Li,[1] G. Li,[2] H. B. Li,[1,‡] H. H. Li,[1] J. Li,[1] J. C. Li,[1] Q. J. Li,[1] R. Y. Li,[1] S. M. Li,[1] W. D. Li,[1] W. G. Li,[1] X. L. Li,[8] X. Q. Li,[10] Y. L. Li,[4] Y. F. Liang,[14] H. B. Liao,[6] C. X. Liu,[1] F. Liu,[6] Fang Liu,[17] H. H. Liu,[1] H. M. Liu,[1] J. Liu,[11] J. B. Liu,[1] J. P. Liu,[18] R. G. Liu,[1] Z. A. Liu,[1] Z. X. Liu,[1] F. Lu,[1] G. R. Lu,[5] H. J. Lu,[17] J. G. Lu,[1] C. L. Luo,[9] L. X. Luo,[4] X. L. Luo,[1] F. C. Ma,[8] H. L. Ma,[1] J. M. Ma,[1] L. L. Ma,[1] Q. M. Ma,[1] X. B. Ma,[5] X. Y. Ma,[1] Z. P. Mao,[1] X. H. Mo,[1] J. Nie,[1] Z. D. Nie,[1] S. L. Olsen,[16] H. P. Peng,[17] N. D. Qi,[1] C. D. Qian,[13] H. Qin,[9] J. F. Qiu,[1] Z. Y. Ren,[1] G. Rong,[1] L. Y. Shan,[1] L. Shang,[1] D. L. Shen,[1] X. Y. Shen,[1] H. Y. Sheng,[1] F. Shi,[1] X. Shi,[11,§] H. S. Sun,[1] J. F. Sun,[1] S. S. Sun,[1] Y. Z. Sun,[1] Z. J. Sun,[1] X. Tang,[1] N. Tao,[17] Y. R. Tian,[15] G. L. Tong,[1] G. S. Varner,[16] D. Y. Wang,[1] J. Z. Wang,[1] K. Wang,[17] L. Wang,[1] L. S. Wang,[1] M. Wang,[1] P. Wang,[1] P. L. Wang,[1] S. Z. Wang,[1] W. F. Wang,[1,‖] Y. F. Wang,[1] Z. Wang,[1] Z. Y. Wang,[1] Zhe Wang,[1] Zheng Wang,[2] C. L. Wei,[1] D. H. Wei,[1] N. Wu,[1] Y. M. Wu,[1] X. M. Xia,[1] X. X. Xie,[1] B. Xin,[8,†] G. F. Xu,[1] H. Xu,[1] S. T. Xue,[1] M. L. Yan,[17] F. Yang,[10] H. X. Yang,[1] J. Yang,[17] Y. X. Yang,[3] M. Ye,[1] M. H. Ye,[2] Y. X. Ye,[17] L. H. Yi,[7] Z. Y. Yi,[1] C. S. Yu,[1] G. W. Yu,[1] C. Z. Yuan,[1] J. M. Yuan,[1] Y. Yuan,[1] S. L. Zang,[1] Y. Zeng,[7] Yu Zeng,[1] B. X. Zhang,[1] B. Y. Zhang,[1] C. C. Zhang,[1] D. H. Zhang,[1] H. Y. Zhang,[1] J. Zhang,[1] J. W. Zhang,[1] J. Y. Zhang,[1] Q. J. Zhang,[1] S. Q. Zhang,[1] X. M. Zhang,[1] X. Y. Zhang,[12] Y. Y. Zhang,[1] Yiyun Zhang,[14] Z. P. Zhang,[17] Z. Q. Zhang,[5] D. X. Zhao,[1] J. B. Zhao,[1] J. W. Zhao,[1] M. G. Zhao,[10] P. P. Zhao,[1] W. R. Zhao,[1] X. J. Zhao,[1] Y. B. Zhao,[1] Z. G. Zhao,[1,¶] H. Q. Zheng,[11] J. P. Zheng,[1] L. S. Zheng,[1] Z. P. Zheng,[1] X. C. Zhong,[1] B. Q. Zhou,[1] G. M. Zhou,[1] L. Zhou,[1] N. F. Zhou,[1] K. J. Zhu,[1] Q. M. Zhu,[1] Y. C. Zhu,[1] Y. S. Zhu,[1] Yingchun Zhu,[1,**] Z. A. Zhu,[1] B. A. Zhuang,[1] X. A. Zhuang,[1] and B. S. Zou[1]

(BES Collaboration)

[1]*Institute of High Energy Physics, Beijing 100049, People's Republic of China*
[2]*China Center for Advanced Science and Technology (CCAST), Beijing 100080, People's Republic of China*
[3]*Guangxi Normal University, Guilin 541004, People's Republic of China*
[4]*Guangxi University, Nanning 530004, People's Republic of China*
[5]*Henan Normal University, Xinxiang 453002, People's Republic of China*
[6]*Huazhong Normal University, Wuhan 430079, People's Republic of China*
[7]*Hunan University, Changsha 410082, People's Republic of China*
[8]*Liaoning University, Shenyang 110036, People's Republic of China*
[9]*Nanjing Normal University, Nanjing 210097, People's Republic of China*
[10]*Nankai University, Tianjin 300071, People's Republic of China*
[11]*Peking University, Beijing 100871, People's Republic of China*
[12]*Shandong University, Jinan 250100, People's Republic of China*
[13]*Shanghai Jiaotong University, Shanghai 200030, People's Republic of China*
[14]*Sichuan University, Chengdu 610064, People's Republic of China*
[15]*Tsinghua University, Beijing 100084, People's Republic of China*
[16]*University of Hawaii, Honolulu, Hawaii 96822, USA*
[17]*University of Science and Technology of China, Hefei 230026, People's Republic of China*
[18]*Wuhan University, Wuhan 430072, People's Republic of China*
[19]*Zhejiang University, Hangzhou 310028, People's Republic of China*
(Received 23 March 2005; published 6 July 2005)

*Current address: Iowa State University, Ames, IA 50011-3160, USA.
†Current address: Purdue University, West Lafayette, IN 47907, USA.
‡Current address: University of Wisconsin at Madison, Madison, WI 53706, USA.
§Current address: Cornell University, Ithaca, NY 14853, USA.
‖Current address: Laboratoire de l'Accélératear Linéaire, F-91898 Orsay, France.
¶Current address: University of Michigan, Ann Arbor, MI 48109, USA.
**Current address: DESY, D-22607, Hamburg, Germany.

Using data samples collected at $\sqrt{s} = 3.686$ GeV and 3.650 GeV by the BESII detector at the BEPC, the branching fraction of $\psi(2S) \to 3(\pi^+\pi^-)$ is measured to be $[5.45 \pm 0.42(\text{stat}) \pm 0.87(\text{syst})] \times 10^{-4}$, and the relative branching fraction of $J/\psi \to 2(\pi^+\pi^-)$ to that of $J/\psi \to \mu^+\mu^-$ is measured to be $[6.01 \pm 0.20(\text{stat}) \pm 0.48(\text{syst})]\%$ via $\psi(2S) \to \pi^+\pi^- J/\psi, J/\psi \to 2(\pi^+\pi^-)$. The electromagnetic form factor of $3(\pi^+\pi^-)$ is determined to be 0.19 ± 0.02 and 0.24 ± 0.02 at $\sqrt{s} = 3.650$ GeV and 3.686 GeV, respectively.

DOI: 10.1103/PhysRevD.72.012002 PACS numbers: 13.25.Gv, 13.40.Gp, 14.40.Gx

I. INTRODUCTION

Strong decays of $\psi(2S)$ to $3(\pi^+\pi^-)$ are suppressed, since the reaction violates G-parity conservation. In e^+e^- colliding beam experiments, $3(\pi^+\pi^-)$ may also be produced by $e^+e^- \to \gamma^* \to 3(\pi^+\pi^-)$ (called the "continuum process" hereafter). It is expected that the continuum contribution is large and may contribute around 60% of the $3(\pi^+\pi^-)$ events at the $\psi(2S)$ energy. This contribution must be removed in determining $\mathcal{B}(\psi(2S) \to 3(\pi^+\pi^-))$, as has been described for the $\psi(2S) \to \pi^+\pi^-$ decay mode [1].

In this analysis, data samples at the $\psi(2S)$ peak ($\sqrt{s} = 3.686$ GeV) and off-resonance ($\sqrt{s} = 3.650$ GeV) are used. The continuum contribution at the $\psi(2S)$ peak is estimated using the off-resonance sample and subtracted to obtain a model-independent measurement of the $\psi(2S) \to 3(\pi^+\pi^-)$ branching fraction. We also use the samples to obtain the $3(\pi^+\pi^-)$ electromagnetic form factor which allows us to calculate the branching fraction based on the theoretical assumption described in Ref. [1].

There is a big contribution from $\psi(2S) \to \pi^+\pi^- J/\psi$, $J/\psi \to 2(\pi^+\pi^-)$ in our $\psi(2S) \to 3(\pi^+\pi^-)$ sample, which allows us to measure the branching fraction of $J/\psi \to 2(\pi^+\pi^-)$. The advantage of this method is that we need not subtract the continuum contribution for this process.

The existing branching fraction measurement of $\psi(2S) \to 3(\pi^+\pi^-)$ was done by the Mark-I experiment [2] based on (9 ± 5) candidate events. The branching fraction of $J/\psi \to 2(\pi^+\pi^-)$ was also measured by Mark-I [3] with (76 ± 9) events observed, and there is also a recent result for this decay reported by the *BABAR* experiment [4].

II. THE BES EXPERIMENT

The data used for this analysis are taken with the updated Beijing Spectrometer (BESII) detector at the Beijing Electron-Positron Collider (BEPC) storage ring. The $\psi(2S)$ data are taken at $\sqrt{s} = 3.686$ GeV with a luminosity of $\mathcal{L}_{3.686} = (19.72 \pm 0.86)$ pb^{-1} [5] measured with large angle Bhabha events. The number of $\psi(2S)$ events is $N^{\text{tot}}_{\psi(2S)} = (14.0 \pm 0.6) \times 10^6$ [6] as determined from inclusive hadrons. The continuum data are taken at $\sqrt{s} = 3.650$ GeV, and the corresponding luminosity is $\mathcal{L}_{3.650} = (6.42 \pm 0.24)$ pb^{-1} [5]. The ratio of the two luminosities is $\mathcal{L}_{3.686}/\mathcal{L}_{3.650} = 3.07 \pm 0.09$.

The BESII detector is a conventional solenoidal magnet detector that is described in detail in Refs. [7,8]. A 12-layer vertex chamber (VC) surrounding the beam pipe provides trigger and track information. A 40-layer main drift chamber (MDC), located radially outside the VC, provides trajectory and energy loss (dE/dx) information for charged tracks over 85% of the total solid angle. The momentum resolution is $\sigma_p/p = 0.017\sqrt{1 + p^2}$ (p in GeV/c), and the dE/dx resolution for hadron tracks is $\sim$8%. An array of 48 scintillation counters surrounding the MDC measures the time-of-flight (TOF) of charged tracks with a resolution of $\sim$200 ps for hadrons. Radially outside the TOF system is a 12 radiation length, lead-gas barrel shower counter (BSC). This measures the energies of electrons and photons over $\sim$80% of the total solid angle with an energy resolution of $\sigma_E/E = 22\%/\sqrt{E}$ (E in GeV). Outside of the solenoidal coil, which provides a 0.4 Tesla magnetic field over the tracking volume, is an iron flux return that is instrumented with three double layers of counters that identify muons of momentum greater than 0.5 GeV/c.

A GEANT3-based Monte Carlo (MC) program with detailed consideration of detector performance (such as dead electronic channels) is used to simulate the BESII detector. The consistency between data and Monte Carlo has been carefully checked in many high purity physics channels, and the agreement is quite reasonable [9].

In generating MC samples, initial state radiation is included, and $1/s$ or $1/s^2$ dependent form factors are assumed where required. MC samples of $\psi(2S) \to \pi^+\pi^- J/\psi$, $J/\psi \to X$ are generated with the correct $\pi^+\pi^-$ mass distribution [10], and $\psi(2S) \to \pi^+\pi^- J/\psi$, $J/\psi \to \mu^+\mu^-$ is generated with the correct $\mu^+\mu^-$ angular distribution. Other samples are generated according to phase space.

III. MEASUREMENT OF $\psi(2S) \to 3(\pi^+\pi^-)$

A. Event selection

Six charged tracks with net charge zero are required. Each charged track, reconstructed using hits in the MDC, must have a good helix fit in order to ensure a correct error matrix in the kinematic fit. All six tracks are required to (1) originate from the beam intersection region, i.e. $\sqrt{V_x^2 + V_y^2} < 2$ cm and $|V_z| < 20$ cm, where V_x, V_y, and V_z are the x, y, and z coordinates of the point of closest approach to the interaction point, (2) have $P_{xy} > 0.05$ GeV/c, where P_{xy} is the momentum of the track

transverse to the beam direction, and (3) have $|\cos\theta| \leq 0.8$, where θ is the polar angle of the track.

A four-constraint kinematic fit is performed with the six charged tracks assuming all of them to be pions. If the confidence level of the fit is greater than 1%, the event is categorized as $\psi(2S) \to 3(\pi^+\pi^-)$. Most events with one or more kaons interpreted as pions are removed by this criterion, as are events with extra neutral tracks.

Figure 1 shows the invariant and recoil mass distributions of $\pi^+\pi^-$ pairs. If the recoil mass of any $\pi^+\pi^-$ pair is between 3.06 and 3.14 GeV/c^2, the event is considered a $\psi(2S) \to \pi^+\pi^- J/\psi$, $J/\psi \to 2(\pi^+\pi^-)$ candidate and removed. If the masses of any two $\pi^+\pi^-$ pairs are between 0.47 and 0.53 GeV/c^2, the event is considered as $\psi(2S) \to K^0_S K^0_S \pi^+\pi^-$, $K^0_S \to \pi^+\pi^-$ background and removed.

Applying these criteria to the data collected at $\sqrt{s} = 3.686$ GeV, 671 events survive, while for the data collected at $\sqrt{s} = 3.650$ GeV, 71 events remain. The efficiencies of these criteria are $\varepsilon_{\psi(2S)} = 6.53\%$ for $\psi(2S) \to 3(\pi^+\pi^-)$ and $\varepsilon_{\rm cont} = 4.65\%$ for $e^+e^- \to 3(\pi^+\pi^-)$. The lower $\varepsilon_{\rm cont}$ results from the initial state radiation correction [11] in the generator, which reduces the center-of-mass energy for many events generated. These events cannot survive the kinematic fit, which leads to the lower $\varepsilon_{\rm cont}$.

Remaining backgrounds in the $\psi(2S)$ sample include: (1) residual $K^0_S K^0_S \pi^+\pi^-$ or $\psi(2S) \to \pi^+\pi^- J/\psi$ events; (2) events with kaons or electrons misidentified as pions; and (3) events with low energy neutral tracks like π^0 or γ. Monte Carlo simulations indicate that $N^{\rm bg} = 4.9 \pm 0.7$ events of these backgrounds survive the above selection criteria, which will be subtracted from the observed number of events in the calculation of the branching fraction. Background remaining in the continuum data sample is negligible.

Figure 2 shows the confidence level distribution from the kinematic fitting. The consistency between data and MC is satisfactory except for the first few bins in both Figs. 2(a) and 2(b). Figure 2(a) is similar to the situation for $J/\psi \to 2(\pi^+\pi^-)$ (see Fig. 5). Taking into account the similarity between the figures and that we expect little background in Fig. 5, we conclude that the discrepancy is due to the simulation of the error matrix in the track fitting rather than some unknown background, and this effect is included in the systematic error analysis.

B. Branching fraction and systematic error

To obtain the branching fraction for $\psi(2S) \to 3(\pi^+\pi^-)$, we have to subtract from $N^{\rm obs}_{3.686}$ the number of continuum events at 3.686 GeV. This number is estimated as $N^{\rm obs}_{3.650} \times f$, where f is the normalization factor:

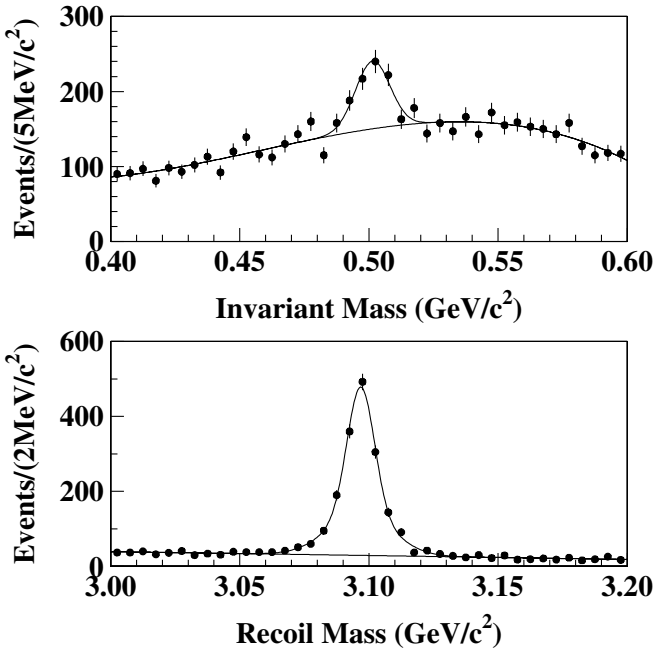

FIG. 1. The $\pi^+\pi^-$ invariant and recoil mass distributions of $\psi(2S) \to 3(\pi^+\pi^-)$ candidates at $\sqrt{s} = 3.686$ GeV. The events with the invariant masses of two $\pi^+\pi^-$ pairs within (0.47, 0.53) GeV/c^2 are removed as $K^0_S K^0_S$ background. The events with the recoil mass of a $\pi^+\pi^-$ pair within (3.06, 3.14) GeV/c^2 are removed as $\psi(2S) \to \pi^+\pi^- J/\psi$ background.

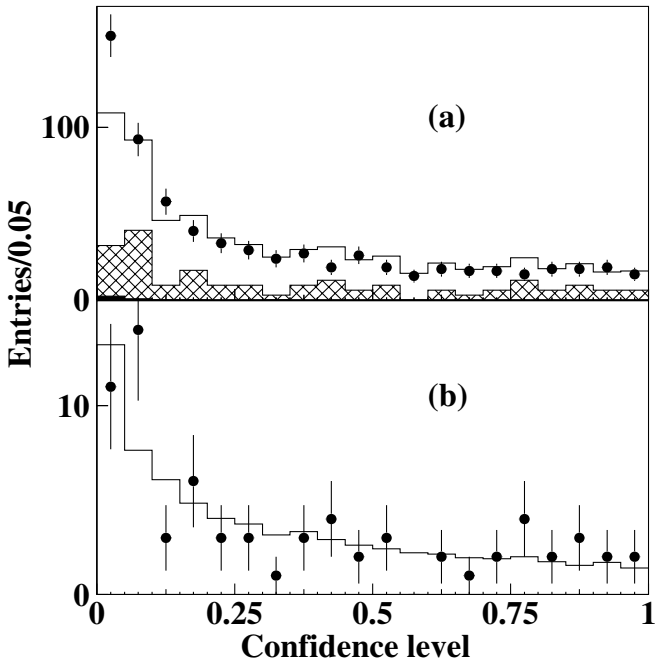

FIG. 2. Confidence level distribution from the kinematic fitting. (a) is for $\psi(2S) \to 3(\pi^+\pi^-)$. The dots with error bars are data. The blank histogram is the MC simulated signal plus the continuum contribution measured with $\sqrt{s} = 3.650$ GeV data (hatched histogram) and the MC simulated background events (dark shaded histogram), after proper normalization. (b) is for $e^+e^- \to 3(\pi^+\pi^-)$ measured with $\sqrt{s} = 3.650$ GeV data. The dots with error bars are data, while the blank histogram is MC simulation.

$$f = \frac{\mathcal{L}_{3.686} \times \sigma^{\rm cont}_{3.686}}{\mathcal{L}_{3.650} \times \sigma^{\rm cont}_{3.650}},$$

where $\sigma^{\rm cont}$ is the Born order cross section of continuum process, which is s dependent and can be expressed in terms of the $3(\pi^+\pi^-)$ form factor $\mathcal{F}(s)$:

$$\sigma^{\rm cont}(s) = \frac{4\pi\alpha^2}{3s} \times |\mathcal{F}(s)|^2, \quad (1)$$

where α is the QED fine structure constant. Assuming $\mathcal{F}(s) \propto 1/s$, we get

$$f = \frac{\mathcal{L}_{3.686}}{\mathcal{L}_{3.650}} \times \left(\frac{3.650}{3.686}\right)^6 = \frac{\mathcal{L}_{3.686}}{\mathcal{L}_{3.650}} \times 0.94.$$

Since an isotropic MC simulation is used to estimate the efficiency, we must correct the efficiency if the real angular distribution deviates from isotropy. Figure 3 shows the angular distribution of all tracks in the data sample (dots with error bars), as well as that from the MC simulation (histogram). The good agreement indicates that the MC simulation assuming isotropy is not a bad approximation to the real situation.

After dividing the angular distribution of data by that of the MC simulation, the efficiency-corrected angular distribution is obtained. Using $1 + \alpha\cos^2\theta$ to fit this corrected distribution, we obtain $\alpha = 0.11 \pm 0.10$. To correct for this deviation from isotropy, we must multiply $\varepsilon_{\psi(2S)}$ by a correction factor, $g = 92.6\% \times (1 \pm 0.07)$.

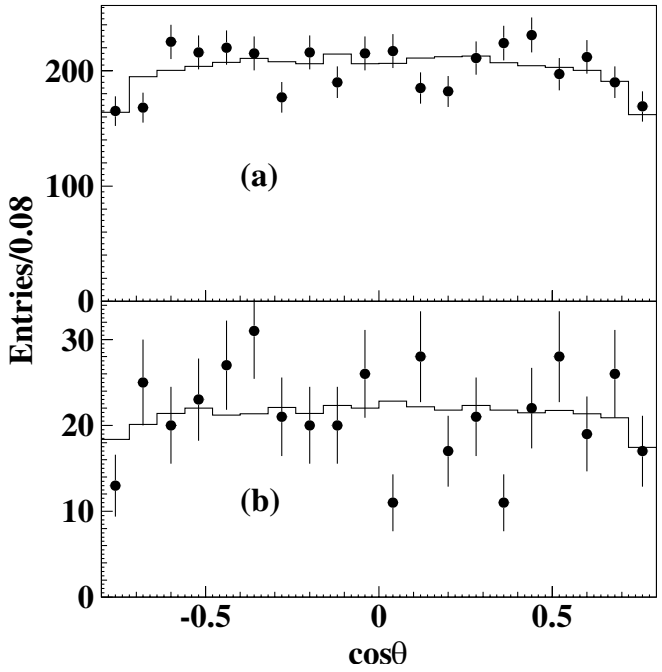

FIG. 3. Distributions of $\cos\theta$ for all the tracks. (a) is for $\psi(2S) \to 3(\pi^+\pi^-)$. (b) is for $e^+e^- \to 3(\pi^+\pi^-)$ measured with $\sqrt{s} = 3.650$ GeV data. The dots with error bars are data. The histograms are the MC simulations.

TABLE I. Numbers used to calculate $\mathcal{B}[\psi(2S) \to 3(\pi^+\pi^-)]$.

$N^{\rm obs}_{3.686}$	$N^{\rm obs}_{3.650}$	f	$N^{\rm bg}$	$\varepsilon_{\psi(2S)}$	g	$N^{\rm tot}_{\psi(2S)}$
671	71	3.07×0.94	4.9	6.53%	92.6%	1.4×10^7

The branching fraction of $\psi(2S) \to 3(\pi^+\pi^-)$ can be calculated as

$$\mathcal{B}[\psi(2S) \to 3(\pi^+\pi^-)] = \frac{N^{\rm obs}_{3.686} - (N^{\rm obs}_{3.650} \times f) - N^{\rm bg}}{(\varepsilon_{\psi(2S)} \times g) \times N^{\rm tot}_{\psi(2S)}} = (5.45 \pm 0.42 \pm 0.87) \times 10^{-4},$$

where the first error is statistical and the second is systematic. The values of the variables in the equation are listed in Table I.

The systematic errors come mainly from the angular distribution, the MDC tracking, the generator, the continuum subtraction, and the kinematic fit, as well as the statistics of the MC samples. The systematic error contributions are listed in Table II and explained below. The total systematic error is 16%.

(1) Since the angular distribution of data deviates from isotropy, the efficiency is multiplied by a correction factor g, which has an uncertainty of 7%.

(2) The MDC tracking efficiency was measured using $J/\psi \to \Lambda\bar{\Lambda}$ and $\psi(2S) \to \pi^+\pi^- J/\psi$, $J/\psi \to \mu^+\mu^-$ events. It is found that the MC simulation agrees with data within 1%–2% for each charged track. The largest difference is taken as a conservative estimation, and 12% is quoted as the systematic error on the tracking efficiency for the channel of interest.

(3) Figure 4 shows the $\pi^+\pi^-$ mass distributions after applying all the selection criteria; a clear ρ signal is observed in both the $\psi(2S)$ and the continuum samples. To estimate the efficiency difference between the data and MC simulation (pure phase space), we generate samples with different intermediate states in $\psi(2S) \to 3(\pi^+\pi^-)$, e.g., ρ, ω, etc., and find the differences from pure phase space are at the 4% and 5% level for $\psi(2S)$ decays and

TABLE II. Summary of systematic errors for $\mathcal{B}[\psi(2S) \to 3(\pi^+\pi^-)]$.

Source	Systematic error (%)
Angular distribution	7
MDC tracking	12
Generator	4
Continuum subtraction	2
Kinematic fit	4
MC statistics	0.7
Total number of $\psi(2S)$	4
Total	16

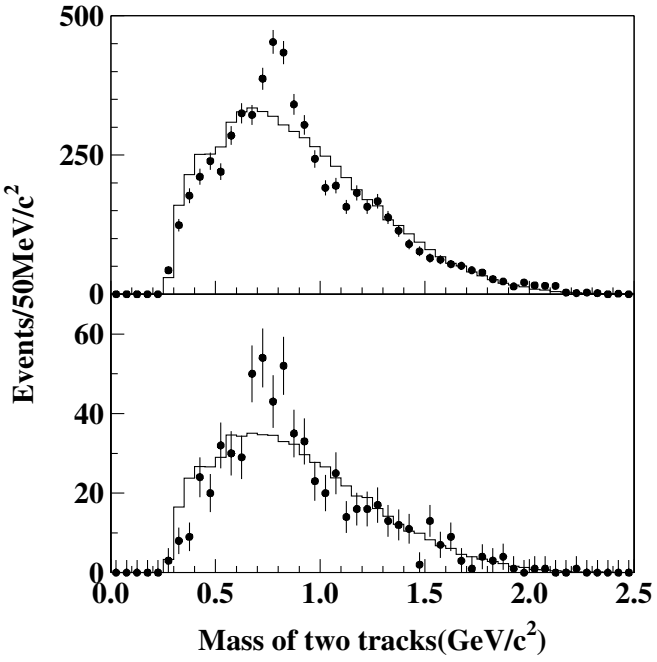

FIG. 4. The $\pi^+\pi^-$ invariant mass distributions after applying all selection criteria. The upper plot is for $\psi(2S) \to 3(\pi^+\pi^-)$, while the lower one is for $e^+e^- \to 3(\pi^+\pi^-)$. The dots with error bars are data, while the histograms are MC simulated phase space distributions. All $\pi^+\pi^-$ combinations are included.

continuum data, respectively, which are taken as the systematic errors from the generator.

(4) Above, we assumed $\mathcal{F}(s) \propto 1/s$ when subtracting the continuum contribution. Assuming a different dependence, such as $\mathcal{F}(s) \propto 1/s^2$, yields a difference of 2% and is regarded as the systematic error of the continuum subtraction.

(5) The systematic uncertainty from the kinematic fit is estimated to be around 4% by using a different MDC wire resolution simulation model [9]. This is in agreement with various studies using pure data samples which can be selected without using a kinematic fit [14].

Compared to the previous Mark-I result [2] of $\mathcal{B}[\psi(2S) \to 3(\pi^+\pi^-)] = (1.5 \pm 1.0) \times 10^{-4}$, our measurement has much better precision and a considerably higher central value.

C. Form factor of $e^+e^- \to 3(\pi^+\pi^-)$

Using our values of $N^{\rm obs}_{3.650}$ and $\mathcal{L}$ and Eq. (1), the form factor at $\sqrt{s} = 3.650$ GeV can be determined. Following the procedure in Ref. [1], assuming only one photon annihilation in $\psi(2S) \to 3(\pi^+\pi^-)$ decays, one can also determine the form factor at $\sqrt{s} = 3.686$ GeV, using [1]

$$\sigma_{\rm Born}(s) = \frac{4\pi\alpha^2}{3s} \times |\mathcal{F}(s)|^2 \times [1 + 2\mathcal{R}B(s) + |B(s)|^2] \approx \frac{4\pi\alpha^2}{3s} \times |\mathcal{F}(s)|^2 \times [1 + |B(s)|^2], \quad (2)$$

with

$$B(s) = \frac{3\sqrt{s}\Gamma_{ee}/\alpha}{s - M^2_{\psi(2S)} + iM_{\psi(2S)}\Gamma_t},$$

where $M_{\psi(2S)}$ is the mass of $\psi(2S)$ and Γ_{ee} and Γ_t are the partial width to e^+e^- and total width of $\psi(2S)$. In Eq. (2), the interference term is neglected since it is at the 1.3% level [1] and small compared with the experimental uncertainties.

Using the numbers listed in Table I, we obtain

$$|\mathcal{F}(s = (3.650\ \text{GeV})^2)| = 0.19 \pm 0.02,$$
$$|\mathcal{F}(s = (3.686\ \text{GeV})^2)| = 0.24 \pm 0.02.$$

The form factor measured at $\sqrt{s} = 3.686$ GeV is larger than that measured at $\sqrt{s} = 3.650$ GeV, which implies that there might be some contribution other than from the electromagnetic interaction in $\psi(2S)$ decays.

Using the form factor measured at the $\psi(2S)$ peak, the branching fraction of $\psi(2S) \to 3(\pi^+\pi^-)$ is determined to be

$$\mathcal{B}[\psi(2S) \to 3(\pi^+\pi^-)] = (4.3 \pm 0.6) \times 10^{-4},$$

which is smaller than the result obtained by subtracting the continuum contribution determined from the continuum data. In the above calculations, $|\mathcal{F}(s)| \propto 1/s$ is assumed; assuming $|\mathcal{F}(s)| \propto 1/s^2$ results in a difference in $\mathcal{B}[\psi(2S) \to 3(\pi^+\pi^-)]$ less than 4%, which is taken as a systematic error in this branching fraction.

IV. MEASUREMENT OF $J/\psi \to 2(\pi^+\pi^-)$

As has been shown in Fig. 1, $\psi(2S) \to 3(\pi^+\pi^-)$ final states can be used to measure the branching fraction of $J/\psi \to 2(\pi^+\pi^-)$ via $\psi(2S) \to \pi^+\pi^- J/\psi$, $J/\psi \to 2(\pi^+\pi^-)$. In order to decrease the systematic error, we determine the branching fraction of $J/\psi \to 2(\pi^+\pi^-)$ from a comparison of the following two processes as has been done in Ref. [14]:

$$\psi(2S) \to \pi^+\pi^- J/\psi,\ J/\psi \to 2(\pi^+\pi^-) \quad \text{(I)}$$

$$\psi(2S) \to \pi^+\pi^- J/\psi,\ J/\psi \to \mu^+\mu^- \quad \text{(II)}$$

The branching fraction is determined from

$$\mathcal{B}[J/\psi \to 2(\pi^+\pi^-)] = \frac{N^{\rm obs}_{\rm I}/\varepsilon_{\rm I}}{N^{\rm obs}_{\rm II}/\varepsilon_{\rm II}} \times \mathcal{B}(J/\psi \to \mu^+\mu^-),$$

where $N^{\rm obs}$ is the number of observed events, and ε is the efficiency. The branching fraction for the leptonic decay $J/\psi \to \mu^+\mu^-$ is obtained from the PDG [15].

A. Event selection

For process I, we use the same selection criteria as for $\psi(2S) \to 3(\pi^+\pi^-)$ except the $\pi^+\pi^- J/\psi$ and $K^0_S K^0_S \pi^+\pi^-$

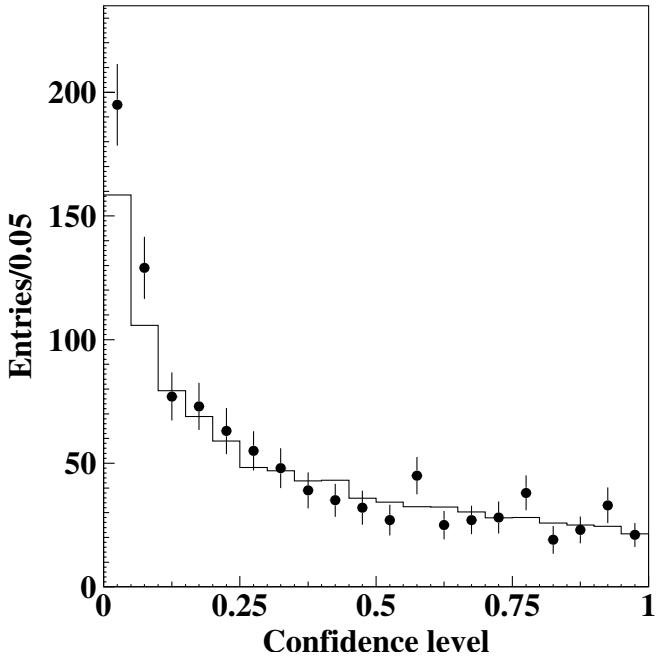

FIG. 5. The confidence level distribution for kinematic fitting of $\psi(2S) \to \pi^+\pi^- J/\psi$, $J/\psi \to 2(\pi^+\pi^-)$ events. The dots with error bars are data, while the blank histogram is the MC simulated signal.

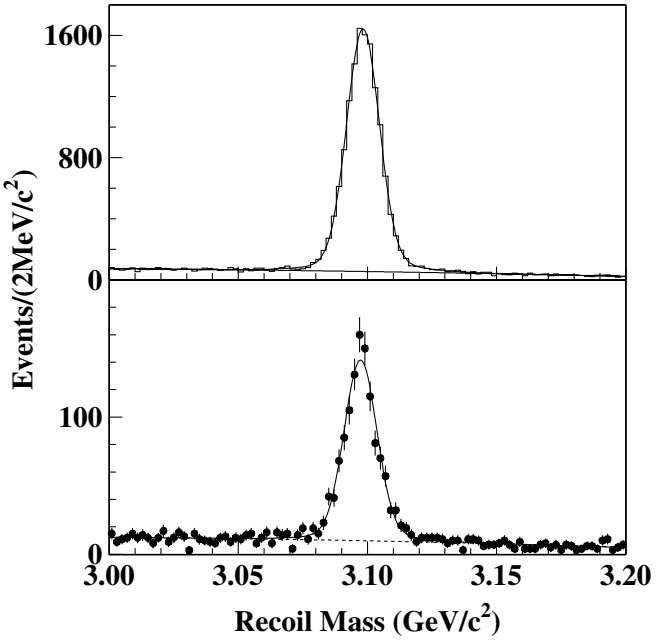

FIG. 6. $\pi^+\pi^-$ recoil mass distributions of $\psi(2S) \to 3(\pi^+\pi^-)$ candidates. The histogram is the MC simulation (upper plot), while the dots with error bars are data (lower plot). The smooth curves show the best fits to the distributions as described in the text. All $\pi^+\pi^-$ combinations are included, and the background mainly comes from the incorrect combinations.

vetoes are no longer used. In addition, to remove $\psi(2S) \to \pi^+\pi^- J/\psi$, $J/\psi \to K^*\overline{K}$ + c.c. $\to K^0_S K^+\pi^-$ + c.c. background, events are vetoed if the recoil mass of one $\pi^+\pi^-$ pair falls into $(3.07, 3.12)$ GeV/c^2 and, at the same time, the mass of another $\pi^+\pi^-$ pair falls into $(0.47, 0.53)$ GeV/c^2.

Figure 5 shows confidence level distributions for the kinematic fitting of $\psi(2S) \to \pi^+\pi^- J/\psi$, $J/\psi \to 2(\pi^+\pi^-)$. The agreement between data and MC simulation is very similar to that of direct $\psi(2S) \to 3(\pi^+\pi^-)$ in Fig. 2(a). Because of the clean J/ψ signal seen below, we may conclude that there is nearly no background in this process and that the discrepancy at small confidence level is due to the simulation of the error matrix in track fitting, which will be taken into consideration in the systematic error.

For process II, the selection criteria are similar to those in Ref. [10]. The two lower momentum tracks are assumed to be $\pi^+\pi^-$, while the two higher momentum tracks $\mu^+\mu^-$. The recoil mass of $\pi^+\pi^-$ candidates must fall within $(3.0, 3.2)$ GeV/c^2, while the invariant mass of $\mu^+\mu^-$ candidates must be within 250 MeV/c^2 of the J/ψ mass. For $\mu^+\mu^-$ candidates, each track must have $N^{\rm hit} \geq 2$, where $N^{\rm hit}$ is the number of muon identification (MUID) layers with matched hits and ranges from 0 to 3, indicating not a muon (0) or a weakly (1), moderately (2), or strongly (3) identified muon [16].

The recoil mass distribution of all $\pi^+\pi^-$ combinations of $\psi(2S) \to 3(\pi^+\pi^-)$ candidate events is shown in Fig. 6. Both data and MC simulation are fitted using a double-Gaussian for the J/ψ signal and a second order polynomial for the background. Figure 7 shows the $\pi^+\pi^-$ recoil mass distribution of the $\psi(2S) \to \pi^+\pi^-\mu^+\mu^-$ candidates. A similar fit is performed as for the $3(\pi^+\pi^-)$ mode. From the fits we get $N^{\rm obs}_{\rm I} = 1107 \pm 37$, $N^{\rm obs}_{\rm II} = 47399 \pm 224$, $\varepsilon_{\rm I} = (6.68 \pm 0.07)\%$, and $\varepsilon_{\rm II} = (16.40 \pm 0.14)\%$, where the errors are given by the fits. There are large systematic errors for the efficiencies. However, what we use to calculate the relative branching fraction is the ratio of these two efficiencies. Most errors cancel by this method. Thus, the ratios of $N^{\rm obs}_{\rm I}/N^{\rm obs}_{\rm II}$ and $\varepsilon_{\rm I}/\varepsilon_{\rm II}$ are more reliable.

The efficiency for $\psi(2S) \to \pi^+\pi^- J/\psi$, $J/\psi \to 2(\pi^+\pi^-)$ must also be corrected if the angular distribution of pions in $J/\psi \to 2(\pi^+\pi^-)$ deviates from isotropy; the angular distribution is shown in Fig. 8. The good agreement between data (dots with error bars) and MC (histogram) indicates that the isotropic MC simulation is not a bad approximation.

After dividing the angular distribution of data by that of MC simulation, the efficiency-corrected angular distribution is obtained. Using $1 + \alpha\cos^2\theta$ to fit this corrected distribution, we obtain $\alpha = 0.10 \pm 0.09$ and a correction factor, $g = 95.4\% \times (1 \pm 0.04)$.

B. Branching fraction and systematic error

The relative branching fraction of $J/\psi \to 2(\pi^+\pi^-)$ is determined to be

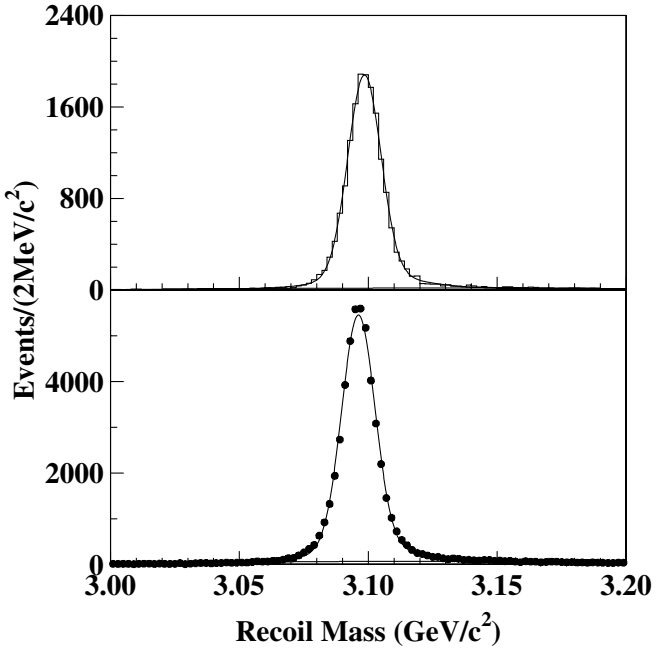

FIG. 7. The $\pi^+\pi^-$ recoil mass distributions of $\psi(2S) \to \pi^+\pi^-\mu^+\mu^-$ candidates. The histogram is the MC simulation (upper plot), while the dots with error bars are data (lower plot). The smooth curves show the best fits to the distributions as described in the text.

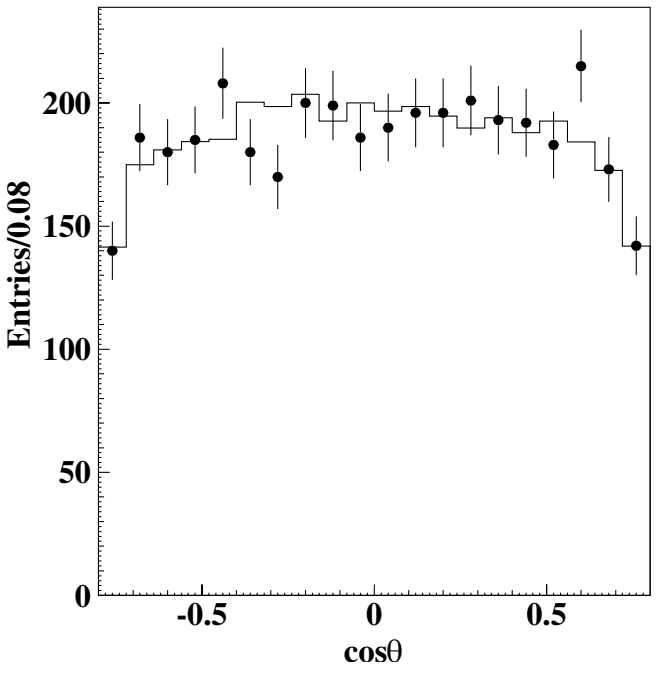

FIG. 8. Distributions of $\cos\theta$ for all the tracks in $J/\psi \to 2(\pi^+\pi^-)$. The dots with error bars are data. The histograms are the MC simulations.

TABLE III. Numbers used to calculate $\mathcal{B}[J/\psi \to 2(\pi^+\pi^-)]/\mathcal{B}[J/\psi \to \mu^+\mu^-]$.

$N_{\rm I}^{\rm obs}$	$N_{\rm II}^{\rm obs}$	$\varepsilon_{\rm I}$	$\varepsilon_{\rm II}$	g
1107	47399	6.68%	16.40%	95.4%

$$\frac{\mathcal{B}[J/\psi \to 2(\pi^+\pi^-)]}{\mathcal{B}[J/\psi \to \mu^+\mu^-]} = \frac{N_{\rm I}^{\rm obs}/(\varepsilon_I \times g)}{N_{\rm II}^{\rm obs}/\varepsilon_{\rm II}} = (6.01 \pm 0.20 \pm 0.48)\%,$$

where the first error is statistical and the second systematic. The values of the variables in the equation are listed in Table III.

Using the branching fraction of $J/\psi \to \mu^+\mu^-$ from the PDG [15], we obtain

$$\mathcal{B}[J/\psi \to 2(\pi^+\pi^-)] = (3.53 \pm 0.12 \pm 0.29) \times 10^{-3}.$$

The error of the branching fraction of $J/\psi \to \mu^+\mu^-$ is included in the systematic error.

Since this is a relative measurement, many systematic errors cancel, either completely or partially. The remaining systematic errors are listed in Table IV and are described below.

(1) The uncertainty in the efficiency due to the uncertainty in the correction factor g, used to account for the deviation from isotropy, is 4%.
(2) For process I, the statistical error of the MC sample is 0.9%, while for process II, it is 0.7%, including any uncertainties introduced by the fits.
(3) There are two more tracks in $J/\psi \to 2(\pi^+\pi^-)$ than in $J/\psi \to \mu^+\mu^-$, the uncertainty in tracking is dominated by the two extra tracks and is estimated to be about 4%.
(4) Figure 9 shows the $\pi^+\pi^-$ mass distributions after all the cuts, where clear ρ and $f_2(1270)$ signals can be seen. To estimate the efficiency difference between data and MC simulation (pure phase space), we generate samples with different intermediate

TABLE IV. Summary of systematic errors for $\mathcal{B}[J/\psi \to 2(\pi^+\pi^-)]/\mathcal{B}[J/\psi \to \mu^+\mu^-]$.

Source	Systematic errors (%)
Angular distribution	4
MC statistics	1
MDC tracking	4
Generator	3
Signal fitting	1
Kinematic fitting	4
Muon identification	2
Background	1
Total error	8

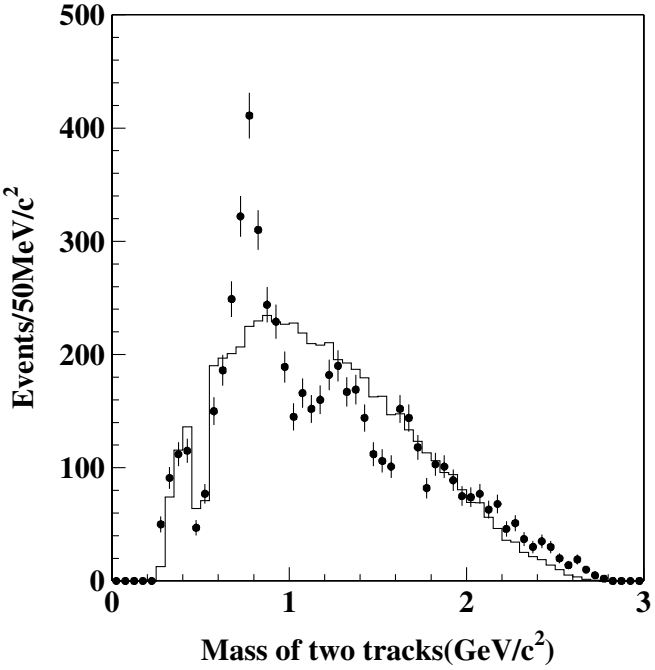

FIG. 9. The $\pi^+\pi^-$ invariant mass distributions for $J/\psi \to 2(\pi^+\pi^-)$ candidates after applying all the selection criteria. The dots with error bars are data, while the histogram is the MC simulated phase space. The dip at the left side of the ρ peak is due to the K^0_S mass cut. There are four entries for each $J/\psi \to 2(\pi^+\pi^-)$ event.

states in $J/\psi \to 2(\pi^+\pi^-)$, e.g., ρ, $f_2(1270)$, $a_2(1320)$, etc., and find the differences from the pure phase space MC simulation are about 3%, which is taken as the systematic error for the generator.

(5) The numbers of events obtained from the fits are affected by the background shape, as well as the signal shape. Using a linear background yields a change of the branching fraction of 1%, while using direct counting methods to estimate the numbers of events and efficiency results in negligible change in the branching fraction. The systematic error due to the fitting procedure is taken as 1%.

(6) The systematic uncertainty from the kinematic fit is estimated the same as that of $\psi(2S) \to 3(\pi^+\pi^-)$ and is about 4%.

(7) Instead of using the MUID, a $\mu^+\mu^-$ sample may be obtained by using the energy deposited in the shower counter to remove $J/\psi \to e^+e^-$ events and neglecting $J/\psi \to \pi^+\pi^-$ and K^+K^- which have small branching ratios [14]. From the number of events obtained with this method, we find that the error associated with the MUID requirement is about 2%.

(8) Background contamination is determined using Monte Carlo simulation. The background fractions in both processes are far less than 1%, and the uncertainty of the estimation is at the 0.5% level.

Adding the systematic errors in quadrature, the total systematic error for $\mathcal{B}[J/\psi \to 2(\pi^+\pi^-)]$ is 8%.

Our measurement of $\mathcal{B}[J/\psi \to 2(\pi^+\pi^-)]$ is in good agreement with the existing measurement by Mark-I [3], which is $(4.0 \pm 1.0) \times 10^{-3}$, based on 76 observed events. Although nonresonance continuum $2(\pi^+\pi^-)$ production was mentioned in the Mark-I paper, it is not clear whether it was removed in evaluating the J/ψ decay branching fraction. Our result has better precision compared with the Mark-I result [3]. A recent measurement of this branching fraction using initial state radiation events was reported by the *BABAR* experiment [4]; the result $[(3.61 \pm 0.26 \pm 0.26) \times 10^{-3}]$ also agrees well with our measurement.

V. SUMMARY

Using 14 M $\psi(2S)$ events and 6.42 pb^{-1} of continuum data at $\sqrt{s} = 3.650$ GeV, the branching fractions of $\psi(2S) \to 3(\pi^+\pi^-)$ and $J/\psi \to 2(\pi^+\pi^-)$ are determined to be $(5.45 \pm 0.42 \pm 0.87) \times 10^{-4}$ and $(3.53 \pm 0.12 \pm 0.29) \times 10^{-3}$, respectively. The former is larger than the Mark-I result using $\psi(2S)$ decays [2], while the latter is consistent with the Mark-I measurement [3] using a J/ψ decay sample. In both cases, our measurements have improved precision.

Using the above results and $\mathcal{B}[\psi(2S) \to 2(\pi^+\pi^-)]$, $\mathcal{B}[J/\psi \to 3(\pi^+\pi^-)]$ from PDG [15], we obtain

$$Q_h \equiv \frac{\mathcal{B}[\psi(2S) \to 3(\pi^+\pi^-)]}{\mathcal{B}[J/\psi \to 3(\pi^+\pi^-)]} = (14 \pm 8)\%,$$

$$Q_h \equiv \frac{\mathcal{B}[\psi(2S) \to 2(\pi^+\pi^-)]}{\mathcal{B}[J/\psi \to 2(\pi^+\pi^-)]} = (13 \pm 3)\%.$$

They are consistent with the ''12% rule'' [17] expectation within errors.

ACKNOWLEDGMENTS

BES Collaboration thanks the staff of BEPC for their hard efforts and the members of IHEP computing center for their helpful assistance. This work is supported in part by the National Natural Science Foundation of China under Contract No. 19991480, No. 10225524, No. 10225525, the Chinese Academy of Sciences under Contract No. KJ 95T-03, the 100 Talents Program of CAS under Contract No. U-11, No. U-24, No. U-25, and the Knowledge Innovation Project of CAS under Contract No. U-602, No. U-34 (IHEP); by the National Natural Science Foundation of China under Contract No. 10175060 (USTC), and No. 10225522 (Tsinghua University); and by the U.S. Department of Energy under Contract No. DE-FG02-04ER41291 (University of Hawaii).

[1] P. Wang, X. H. Mo, and C. Z. Yuan, Phys. Lett. B **557**, 192 (2003).
[2] W. Tanenbaum *et al.* (MARK-I Collaboration), Phys. Rev. D **17**, 1731 (1978).
[3] B. Jean-Marie *et al.* (MARK-I Collaboration), Phys. Rev. Lett. **36**, 291 (1976).
[4] B. Aubert *et al.* (*BABAR* Collaboration), hep-ex/0502025.
[5] S. P. Chi *et al.*, High Energy Phys. and Nucl. Phys. **28**, 1135 (2004).
[6] X. H. Mo *et al.*, High Energy Phys. and Nucl. Phys. **28**, 455 (2004).
[7] J. Z. Bai *et al.* (BES Collaboration), Nucl. Instrum. Methods Phys. Res., Sect. A **344**, 319 (1994).
[8] J. Z. Bai *et al.* (BES Collaboration), Nucl. Instrum. Methods Phys. Res., Sect. A **458**, 627 (2001).
[9] M. Ablikim *et al.* (BES Collaboration), physics/0503001 [Nucl. Instr. Meth. A (to be published)].
[10] J. Z. Bai *et al.* (BES Collaboration), Phys. Rev. D **58**, 092006 (1998).
[11] The efficiency of the continuum events, $\varepsilon_{\rm cont}$, goes down when the maximal energy of the hard radiative photon we set in the generator, $E_\gamma^{\rm max}$, becomes large. $\varepsilon_{\rm cont} = 4.65\%$ is related to $E_\gamma^{\rm max} = 0.7$ GeV. In the calculation of the form factor at $\sqrt{s} = 3.650$ GeV, the efficiency is multiplied by an initial state radiation correction factor, $(1 + \delta)$, which goes up when $E_\gamma^{\rm max}$ becomes large [12,13], but the product of $\varepsilon_{\rm cont}$ and $(1 + \delta)$ keeps unchanged, as does the result of the form factor.
[12] G. Bonneau and F. Martin, Nucl. Phys. **B27**, 381 (1971).
[13] É. A. Kuraev and V. S. Fadin, Sov. J. Nucl. Phys. **41(3)**, 466 (1985).
[14] M. Ablikim *et al.* (BES Collaboration), Phys. Rev. D **70**, 012005 (2004).
[15] S. Eidelman *et al.*, Phys. Lett. B **592**, 1 (2004).
[16] J. Z. Bai *et al.* (BES Collaboration), High Energy Phys. and Nucl. Phys. **20**, 97 (1996).
[17] T. Applequist and D. Politzer, Phys. Rev. Lett. **34**, 43 (1975).